Inorg. Chem. **2008**, *47*, 9238−9247

Syntheses, X-ray Structures, Solid State High-Field Electron Paramagnetic Resonance, and Density-Functional Theory Investigations on Chloro and Aqua Mn^{II} Mononuclear Complexes with Amino-Pyridine Pentadentate Ligands

Christelle Hureau,[†,‡] Sihem Groni,[†] Régis Guillot,[§] Geneviève Blondin,*[,†,⊥] Carole Duboc,[#,▽] and Elodie Anxolabéhère-Mallart*[,†]

Equipe de Chimie Inorganique, Institut de Chimie Moléculaire et des Matériaux d'Orsay, UMR 8182 CNRS, Université Paris-Sud, 91405 Orsay Cedex, France, Institut de Chimie Moléculaire et des Matériaux d'Orsay, UMR 8182 CNRS, Université Paris-Sud, 91405 Orsay Cedex, France, Laboratoire des Champs Magnétiques Intenses, UPR 5021, CNRS, 25 rue des Martyrs, BP 166, 38042 Grenoble Cedex 9, France, and Département de Chimie Moléculaire, UMR 5250, Université Joseph Fourier, BP 53, 38041 Grenoble Cedex 9, France

Received March 28, 2008

The two pentadentate amino-pyridine ligands L_5^2 and L_5^3 (L_5^2 and L_5^3 stand for the *N*-methyl-*N,N′,N′*-tris(2-pyridylmethyl)ethane-1,2-diamine and the *N*-methyl-*N,N′,N′*-tris(2-pyridylmethyl)propane-1,3-diamine, respectively) were used to synthesize four mononuclear Mn^{II} complexes, namely $[(L_5^2)MnCl](PF_6)$ (**1**(PF_6)), $[(L_5^3)MnCl](PF_6)$ (**2**(PF_6)), $[(L_5^2)Mn(OH_2)](BPh_4)_2$ (**3**$(BPh_4)_2$), and $[(L_5^3)Mn(OH_2)](BPh_4)_2$ (**4**$(BPh_4)_2$). The X-ray diffraction studies revealed different configurations for the ligand L_5^n ($n = 2, 3$) depending on the sixth exogenous ligand and/or the counterion. Solid state high-field electron paramagnetic resonance spectra were recorded on complexes **1**−**4** as on previously described mononuclear Mn^{II} systems with tetra- or hexadentate amino-pyridine ligands. Positive and negative axial zero-field splitting (ZFS) parameters *D* were determined whose absolute values ranged from 0.090 to 0.180 cm^{-1}. Density-functional theory calculations were performed unraveling that, in contrast with chloro systems, the spin−spin and spin−orbit coupling contributions to the *D*-parameter are comparable for mixed N,O-coordination sphere complexes.

Introduction

In the living word, manganese ion(s) embedded at the core of metalloproteines play(s) crucial roles in the redox processes to sustain life. Perhaps the most important of all is the Oxygen Evolving Complex (OEC), a Mn_4Ca cluster present at the heart of the Photosystem II that is responsible for the four electron oxidation of water.[1,2] The coordination spheres of the manganese ions in the OEC are not clear yet but are rich in oxygen atoms. The active site of Mn-superoxide dismutases (Mn-SOD) accommodates a single Mn ion that shuffles between the +II and +III oxidation states during the catalytic cycle of the disproportionation of the superoxide ion into hydrogen peroxide and water.[3] The metal ion is in a N_3O_2 trigonal bipyramidal geometry.[4,5] Other mononuclear Mn^{II} proteins have been characterized

* To whom correspondence should be addressed. E-mail: genevieve.blondin@cea.fr (G.B.), eanxolab@icmo.u-psud.fr (E.A.-M.).
† Equipe de Chimie Inorganique, Institut de Chimie Moléculaire et des Matériaux d'Orsay, UMR 8182 CNRS, Université Paris-Sud.
‡ Current address: Laboratoire de Chimie de Coordination, UPR 8241 CNRS, 205, route de Narbonne, 31077 Toulouse Cedex 04, France.
§ Institut de Chimie Moléculaire et des Matériaux d'Orsay, UMR 8182 CNRS, Université Paris-Sud.
⊥ Current address: Laboratoire de Chimie et Biologie des Métaux, UMR 5249 CNRS, iRTSV, Bâtiment C5, CEA, 17 rue des Martyrs, 38054 Grenoble Cedex 9, France.
Laboratoire des Champs Magnétiques Intenses, UPR 5021, CNRS.
▽ Département de Chimie Moléculaire, UMR 5250, Université Joseph Fourier.

(1) Barber, J.; Rutherford, A. W. *Philos. Trans. R. Soc. London, Ser. B* **2008**, *363*, 1125–1303.
(2) Forum discussion, *Inorg. Chem.* **2008** *47*, 1697−1861.
(3) Whittaker, J. W. Manganese Superoxide Dismutase. In *Metal ions in Biological Systems*; Sigel, A., Sigel, H. Eds.; Marcel Dekker, Inc.: New York, 2000; Vol. *37*, pp 587−611.
(4) Schmidt, M.; Meier, B.; Parak, F. *J. Biol. Inorg. Chem.* **1996**, *1*, 532–541.
(5) Sugio, S.; Hiraoka, B. Y.; Yamakura, F. *Eur. J. Biochem.* **2000**, *267*, 3487–3495.

10.1021/ic800551u CCC: $40.75 © 2008 American Chemical Society
Published on Web 09/26/2008

that are redox active such as the oxalate decarboxylase[6−8] and the Barley oxalate oxidase[6,9] or non redox active such as the concanavalin A[10,11] and the fosfomycin resistant metalloglutathione transferase FosA.[12,13] In these examples, the Mn^{II} ion is in a mixed O,N-environment.

Efforts have been put in the past few years to establish magneto-structural correlations.[12,14−22] These studies rely on the paramagnetic character of the Mn^{II} ion ($S = 5/2$) that allows elegant and precise investigations by Electron Paramagnetic Resonance (EPR) spectroscopy. Precise determination of the zero-field splitting (ZFS) effects benefitted from the development of high-field and high-frequency EPR (HF-EPR) spectroscopy. The first studies were performed on dihalide complexes, where the influence of the halide (chloride vs bromide vs iodide) has been investigated.[14−19] Density Functional Theory (DFT) calculations have allowed to rationalize the observed variations, in particular in octahedral complexes presenting either *cis*- or *trans*-configurations.[18]

The goal behind the collection of such basic information is in the long run to correlate magnetic characteristics to reactivity.[21] Undoubtedly, this underlies that more sophisticated synthetic models must be elaborated to replicate the coordination schemes of the manganese ion within the natural systems. Along this line, a recently published study dealt with a series of Mn^{II} complexes presenting a mixed N,O-coordination sphere.[23] The influence of the substituent on the aromatic ring bearing a coordinating group was investigated, and correlations between ZFS parameters and Mn^{III}/Mn^{II} redox potentials were tentatively drawn.

Chart 1. Amino-Pyridine Ligands Used in the Present Study

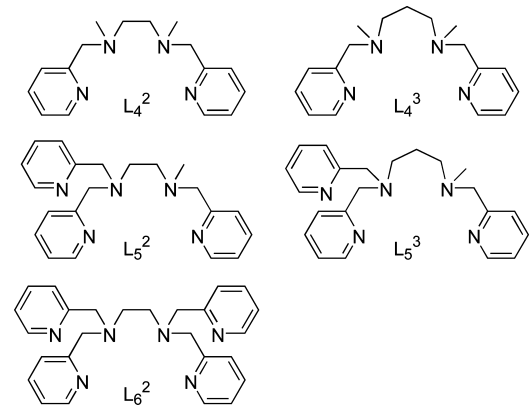

In the present paper, we describe the syntheses and X-ray structures of four mononuclear Mn^{II} complexes obtained with pentadentate amino-pyridine ligands, namely the *N*-methyl-*N,N′,N′*-tris(2-pyridylmethyl)ethane-1,2-diamine (L_5^2) and *N*-methyl-*N,N′,N′*-tris(2-pyridylmethyl)propane-1,3-diamine (L_5^3) (Chart 1). The coordination sphere is completed by either a chloride anion or a water molecule. The L_5^2 and L_5^3 ligands differ in the diamine core leading to a five- or six-membered metallacycle, respectively. These complexes were investigated in the solid state by HF-EPR, and the study was enlarged to previously reported mononuclear Mn^{II} complexes chelated by tetra- or hexadentate amino-pyridine ligands, namely, *cis*-$[(L_4^2)MnCl_2]$ (L_4^2 = *N,N′*-dimethyl-*N,N′*-bis(2-pyridylmethyl)ethane-1,2-diamine),[24] $[(L_4^3)MnCl(OH_2)]^+$ (L_4^3 = *N,N′*-dimethyl-*N,N′*-bis(2-pyridylmethyl)-propane-1,2-diamine),[24] and $[(L_6^2)Mn(OH_2)]^{2+}$ (L_6^2 = *N,N,N′,N′*-tetra(2-pyridylmethyl)ethane-1,2-diamine).[25] The ZFS parameters were analyzed with the help of DFT calculations. This work reports the first HF-EPR studies on monochloro complexes and on a heptacoordinated system. It also presents new data on mixed N,O-coordinated Mn^{II} systems.

Materials and Methods

General Remarks. Reagents and solvents were purchased commercially and used as received.

Syntheses. Ligands L_5^2 and L_5^3. A new three-step route for the synthesis of ligands *N*-methyl-*N,N′,N′*-tris(2-pyridylmethyl)-ethane-1,2-diamine (L_5^2)[26] and *N*-methyl-*N,N′,N′*-tris(2-pyridylmethyl)propane-1,3-diamine (L_5^3)[27] has been investigated (Scheme 1). The absence of a purification step in this new synthesis offers a remarkable advantage compared to the one described by Bernal et al.[28]

(6) Svedruzic, D.; Jónsson, S.; Toyota, C. G.; Reinhardt, L. A.; Ricagno, S.; Lindqvist, Y.; Richards, N. G. J. *Arch. Biochem. Biophys.* **2005**, *433*, 176–192.
(7) Just, V. J.; Stevenson, C. E. M.; Bowater, L.; Tanner, A.; Lawson, D. M.; Bornemann, S. *J. Biol. Chem.* **2004**, *279*, 19867–19874.
(8) Anand, R.; Dorrestein, P. C.; Kinsland, C.; Begley, T. P.; Ealick, S. E. *Biochemistry* **2002**, *41*, 7659–7669.
(9) Woo, E.-J.; Dunwell, J. M.; Goodenough, P. W.; Marvier, A. C.; Pickersgill, R. W. *Nat. Struct. Biol.* **2000**, *7*, 1036–1040.
(10) Kalb (Gilboa), A. J.; Habash, J.; Hunter, N. S.; Price, H. J.; Raftery, J.; Helliwell, J. R. Manganese(II) in concanavalin A and other lectin proteins. In *Metal Ions in Biological Systems*; Sigel, A., Sigel, H. Eds.; Marcel Dekker, Inc: New York, 2000; Vol. *37*, pp 279−304.
(11) Deacon, A.; Gleichmann, T.; Kalb (Gilboa) , A. J.; Price, H.; Raftery, J.; Bradbrook, G.; Yariv, J.; Helliwell, J. R. *J. Chem. Soc., Faraday Trans.* **1997**, *93*, 4305–4312.
(12) Walsby, C. J.; Telser, J.; Rigsby, R. E.; Armstrong, R. N.; Hoffman, B. M. *J. Am. Chem. Soc.* **2005**, *127*, 8310–8319.
(13) Rife, C. L.; Pharris, R. E.; Newcomer, M. E.; Armstrong, R. N. *J. Am. Chem. Soc.* **2002**, *124*, 11001–11003.
(14) Goodgame, D. M. L.; El Mkami, H.; Smith, G. M.; Zhao, J. P.; McInnes, E. J. L. *Dalton Trans.* **2003**, 34–35.
(15) Jacobsen, C. J. H.; Pedersen, E.; Villadsen, J.; Weihe, H. *Inorg. Chem.* **1993**, *32*, 1216–1221.
(16) Lynch, W. B.; Boorse, R. S.; Freed, J. H. *J. Am. Chem. Soc.* **1993**, *115*, 10909–10915.
(17) Wood, R. M.; Stucker, D. M.; Jones, L. M.; Lynch, W. B.; Misra, S. K.; Freed, J. H. *Inorg. Chem.* **1999**, *38*, 5384–5388.
(18) Duboc, C.; Phoeung, T.; Zein, S.; Pécaut, J.; Collomb, M.-N.; Neese, F. *Inorg. Chem.* **2007**, *46*, 4905–4916.
(19) Mantel, C.; Baffert, C.; Romero, I.; Deronzier, A.; Pécaut, J.; Collomb, M.-N.; Duboc, C. *Inorg. Chem.* **2004**, *43*, 6455–6463.
(20) Tabares, L. C.; Cortez, N.; Agalidis, I.; Un, S. *J. Am. Chem. Soc.* **2005**, *127*, 6039–6047.
(21) Smoukov, S. K.; Telser, J.; Bernat, B. A.; Rife, C. L.; Armstrong, R. N.; Hoffman, B. M. *J. Am. Chem. Soc.* **2002**, *124*, 2318–2326.
(22) Duboc, C.; Collomb, M.-N.; Pécaut, J.; Deronzier, A.; Neese, F. *Chem.—Eur. J.* **2008**, *14*, 6498–6509.
(23) Gätjens, J.; Sjödin, M.; Pecoraro, V. L.; Un, S. *J. Am. Chem. Soc.* **2007**, *129*, 13825–13827.
(24) Hureau, C.; Blondin, G.; Charlot, M.-F.; Philouze, C.; Nierlich, M.; Césario, M.; Anxolabéhère-Mallart, E. *Inorg. Chem.* **2005**, *44*, 3669–3683.
(25) Hureau, C.; Blanchard, S.; Nierlich, M.; Blain, G.; Rivière, E.; Girerd, J.-J.; Anxolabéhère-Mallart, E.; Blondin, G. *Inorg. Chem.* **2004**, *43*, 4415–4426.

Scheme 1. Three-Step Synthesis of the L_5^2 and L_5^3 Ligands

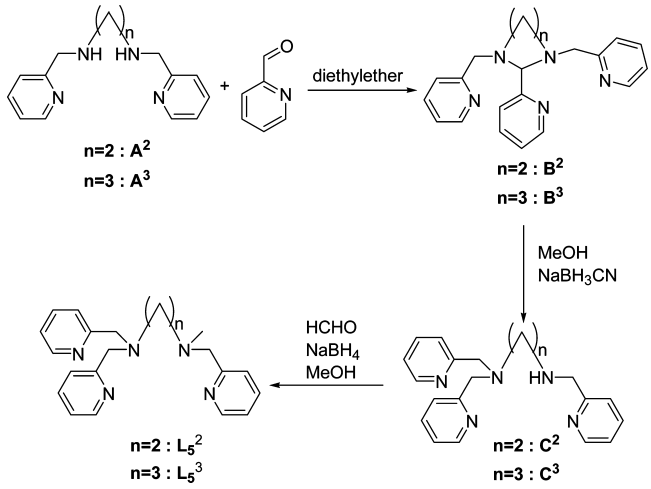

The ligands *N,N′*-bis(2-pyridylmethyl)ethane-1,2-diamine ($\mathbf{A}^2$) and *N,N′*-bis(2-pyridylmethyl)propane-1,3-diamine ($\mathbf{A}^3$) were synthesized as reported earlier.[24]

Step 1: Synthesis of aminal ($\mathbf{B}^2$ and $\mathbf{B}^3$). Twenty millimoles of $\mathbf{A}^2$ (respectively $\mathbf{A}^3$) were dissolved in 100 mL of diethylether. A 1.9 mL quantity (20 mmol) of 2-pyridine-carboxaldehyde was added. The mixture was heated to 80 °C and stirred during 4 h. The methanol was evaporated. The crude product is an orange oil that can be recrystallized from ether. The white solid that precipitated out was filtered on a fritted glass and washed with an ether/methanol (9/1) solution. $\mathbf{B}^2$: 5.5 g, 83% yield; $\mathbf{B}^3$ 4.8 g, 70% yield. $\mathbf{B}^2$:^{1}H NMR (200 MHz, $CDCl_3$, 25 °C): δ = 2.75 (dd, 2H, N-C*Ha*Hb-C*Ha*Hb-N); δ = 3.35 (dd, 2H, N-CHa*Hb*-CHa*Hb*-N); δ = 3.65 (d, 2H, N-C*Ha*Hb-C_5H_4N); δ = 3.95 (d, 2H, N-CHa*Hb*-C_5H_4N); δ = 4.3 (s, 1H, N-C*H*(N)-C_5H_4N); δ = 7.5 (m, 9H, *H*-C_5H_3N); δ = 8.45 (d, 2H, *H*-C_5H_3N), δ = 8.55 (d, 1H, *H*-C_5H_3N). $\mathbf{B}^3$:^{1}H NMR (200 MHz, $CDCl_3$, 25 °C): δ = 1.55 (m, 1H, N-CH_2-C*Ha*Hb-CH_2−N), δ = 1.95 (m, 1H, N-CH_2-CHa*Hb*-CH_2-N), δ = 2.35 (m, 2H, N-C*Ha*Hb-CH_2-C*Ha*Hb-N); δ = 3.05 (m, 2H, N-CHa*Hb*-CH_2-CHa*Hb*-N), δ = 3.35 (d, 2H, N-C*Ha*Hb-C_5H_4N); δ = 3.60 (d, 2H, N-CHa*Hb*-C_5H_4N); δ = 4.05 (s, 1H, N-C*H*(N)-C_5H_4N); δ = 7.5 (m, 9H, *H*-C_5H_3N); δ = 8.45 (d, 2H, *H*-C_5H_3N), δ = 8.55 (d, 1H, *H*-C_5H_3N).

Step 2: *N,N,N′*-tris(2-pyridylmethyl)ethane-1,2-diamine ($\mathbf{C}^2$) and *N,N,N′*-tris(2-pyridylmethyl)propane-1,3-diamine ($\mathbf{C}^3$). Ten millimoles of aminal $\mathbf{B}^2$ (respectively $\mathbf{B}^3$) were dissolved in 100 mL of methanol, and 1.55 mL (20 mmol) of trifluoroacetic acid were added to the pale yellow solution. After cooling in an ice bath, 0.63 g (10 mmol) of sodium cyanoborohydride were slowly added. The mixture was heated to 50 °C and stirred during 2 h. A 100 mL quantity of a solution of 3.75 M NaOH were added after cooling to room temperature. The resulting solution was stirred one additional hour. Methanol was evaporated, and the resulting aqueous solution was extracted with chloroform (3 × 50 mL). Organic phases were gathered, washed with water until the pH of the aqueous phase was 7, dried over anhydrous sodium sulfate and filtered. Solvent was evaporated to give a pale yellow oil. $\mathbf{C}^2$: 2.8 g, 83% yield; $\mathbf{C}^3$ 2.9 g, 85% yield. $\mathbf{C}^2$: ^{1}H NMR (200 MHz, $CDCl_3$, 25 °C): δ = 2.75 (m, 4H, N-C*H*$_2$-C*H*$_2$-N); δ = 3.8 (3s, 6H, N-C*H*$_2$-C_5H_4N); δ = 7.4 (m, 9H, *H*-C_5H_3N); δ = 8.55 (d, 3H, *H*-C_5H_3N). $\mathbf{C}^3$: ^{1}H NMR (200 MHz, $CDCl_3$, 25 °C): δ = 1.8 (q, 2H, N-CH_2-C*H*$_2$-CH_2-N); δ = 2.65 (m, 4H, N-C*H*$_2$-CH_2-C*H*$_2$-N); δ = 3.75 (s, 4H, N-C*H*$_2$-C_5H_4N); δ = 3.85 (s, 2H, N-C*H*$_2$-C_5H_4N)); δ = 7.4 (m, 9H, *H*-C_5H_3N); δ = 8.45 (d, 2H, *H*-C_5H_3N); δ = 8.55 (d, 1H, *H*-C_5H_3N).

Step 3: *N*-methyl-*N,N′,N′*-tris(2-pyridylmethyl)ethane-1,2-diamine (L_5^2) and *N*-methyl-*N,N′,N′*-tris(2-pyridylmethyl)propane-1,3-diamine (L_5^3). Methylation of $\mathbf{C}^2$ and $\mathbf{C}^3$ has been performed according to the method described by Sondengam et al.[29] A 4 mmol quantity of $\mathbf{C}^2$ (respectively $\mathbf{C}^3$) was dissolved in 50 mL of methanol, and 4 mL of an aqueous solution of formaldehyde (70%) was added. The solution was heated under reflux during 30 min. After cooling on an ice bath, 0.4 g of sodium borohydride was added. The mixture was stirred at room temperature for 1 h, and the methanol was evaporated. The yellow oil was taken with 100 mL of distilled water and extracted with chloroform (3 × 25 mL). The organic phases were gathered, dried over anhydrous sodium sulfate and filtered. The solvent was evaporated to give a yellow oil. L_5^2:1.1 g, 78% yield; L_5^3:1.4 g, 97% yield. L_5^2:^{1}H NMR (200 MHz, $CDCl_3$, 25 °C): δ = 2.2 (s, 3H, C*H*$_3$); δ = 2.5 (m, 4H, N-C*H*$_2$-C*H*$_2$-N); δ = 3.6 (s, 2H, N-C*H*$_2$-C_5H_4N); δ = 3.8 (s, 4H, N-C*H*$_2$-C_5H_4N); δ = 7.4 (m, 9H, *H*-C_5H_3N); δ = 8.55 (d, 3H, *H*-C_5H_3N). L_5^3: ^{1}H NMR (200 MHz, $CDCl_3$, 25 °C): δ = 1.8 (q, 2H, N-CH_2-C*H*$_2$-CH_2-N), δ = 2.2 (s, 3H, C*H*$_3$); δ = 2.5 (m, 4H, N-C*H*$_2$-CH_2-C*H*$_2$-N); δ = 3.6 (s, 2H, N-C*H*$_2$-C_5H_4N); δ = 3.8 (s, 4H, N-C*H*$_2$-C_5H_4N); δ = 7.4 (m, 9H, *H*-C_5H_3N); δ = 8.55 (d, 3H, *H*-C_5H_3N).

$[(L_5^2)MnCl](PF_6)\cdot 2H_2O$ ($\mathbf{1}(PF_6)\cdot 2H_2O$). A 694 mg quantity (2.0 mmol) of ligand L_5^2 and 0.39 g (2.0 mmol) of $MnCl_2\cdot 4H_2O$ were mixed in 5 mL of methanol. A slight excess (4.0 mmol) of $NaPF_6$ previously dissolved in 2 mL of methanol was then added to the previous mixture. After filtration, 660 mg (yield = 53%) of a white precipitate was obtained. Crystallization of complex **1** was performed by slow diffusion of ether in an acetonitrile solution of **1**, and crystals of $\mathbf{1}(PF_6)$ suitable for X-ray crystallography study were obtained. Anal. Calcd for $\mathbf{1}(PF_6)\cdot\mathbf{2}H_2O$ (powder) $C_{21}H_{29}ClMnN_5O_2PF_6$: C, 40.8; H, 4.7; N, 11.3. Found: C, 40.2; H, 4.2; N, 11.1. IR: ν (cm^{-1}) = 3461 (S, strong); 2935−2860 (w, weak); 1604 (S); 1571 (m, medium); 1481 (m);1437 (S); 1370 (m); 1314 (m); 1117 (S); 1086 (S); 858 (w); 840 (S); 767 (S); 625 (w); 575 (S); 483 (w); 412(w). ESI-MS: A major peak was detected at *m*/*z* = 437 corresponding to $[(L_5^2)MnCl]^+$.

$[(L_5^3)MnCl](PF_6)$ ($\mathbf{2}(PF_6)$). An identical synthesis was performed using the ligand L_5^3 as starting material and led to 550 mg (yield = 49%) of a white precipitate. Crystallization of complex **2** was performed by slow diffusion of ether in an acetonitrile solution of **2**, and crystals of $\mathbf{2}(PF_6)\cdot 0.5CH_3CN$ suitable for X-ray crystallography study were obtained. Anal. Calcd for $\mathbf{2}(PF_6)$ (powder) $C_{22}H_{27}ClMnN_5PF_6$: C, 44.3; H, 4.6; N, 11.7. Found: C, 44.6; H, 4.7; N, 11.3. IR: ν (cm^{-1}) = 3477 (S, strong); 2959 (w, weak); 1719 (m, medium); 1604 (S); 1573 (m); 1483 (m); 1471 (w); 1437 (S); 1377 (w); 1362 (w); 1298 (w); 1268 (w); 1252 (w); 1220 (w); 1197 (w); 1160 (m); 1137 (S); 1102 (m); 1055 (w); 1048 (w); 1016 (S); 949 (w); 836 (S); 773 (S); 642 (w); 575 (F); 464 (w). ESI-MS: A major peak was detected at *m*/*z* = 451 corresponding to $[(L_5^3)MnCl]^+$.

$[(L_5^2)Mn(OH_2)](BPh_4)_2\cdot 2H_2O$ ($\mathbf{3}(BPh_4)_2\cdot 2H_2O$). A similar synthesis was performed using the ligand L_5^2, $Mn(ClO_4)_2\cdot(H_2O)_6$,

(26) Nivorozhkin, A.; Anxolabéhère-Mallart, E.; Mialane, P.; Davydov, R.; Guilhem, J.; Cesario, M.; Audière, J.-P.; Girerd, J.-J.; Styring, S.; Schussler, L.; Seris, J.-L. *Inorg. Chem.* **1997**, *36*, 846–853.
(27) Balland, V.; Banse, F.; Anxolabéhère-Mallart, E.; Ghiladi, M.; Mattioli, T. A.; Philouze, C.; Blondin, G.; Girerd, J.-J. *Inorg. Chem.* **2003**, *42*, 2470–2477.
(28) Bernal, I.; Jensen, I. M.; Jensen, K. B.; McKenzie, C. J.; Toftlund, H.; Tuchagues, J.-P. *J. Chem. Soc., Dalton Trans.* **1995**, 3667–3675.
(29) Sondengam, B. L.; Hentchoya Hémo, J.; Charles, G. *Tetrahedron Lett.* **1973**, *14*, 261–263.

Table 1. Details of Structure Determination, Refinement, and Experimental Parameters for Compounds **1**(PF_6), **2**(PF_6)·0.5CH_3CN, **3**(BPh_4)$_2$, and **4**(BPh_4)$_2$

	1(PF_6)	**2**(PF_6)·0.5CH_3CN	**3**(BPh_4)$_2$	**4**(BPh_4)$_2$
chemical formula	($C_{21}H_{25}N_5MnCl$), (PF_6)	2($C_{22}H_{27}N_5MnCl$), 2(PF_6), (C_2H_3N)	4($C_{21}H_{27}N_5MnO$), 8($BC_{24}H_{20}$)	($C_{22}H_{29}N_5MnO$), 2($C_{24}H_{20}B$)
formula weight	582.82	1234.75	4227.43	1070.85
crystal system	monoclinic	orthorhombic	triclinic	monoclinic
space group	$P2_1/c$	$P2_12_12_1$	$P1$	Cc
a (Å)	7.7305(4)	16.6295(3)	11.887(3)	15.665(3)
b (Å)	17.8372(12)	17.0758(4)	23.689(6)	17.325(4)
c (Å)	18.2266(12)	18.9529(4)	23.812(7)	21.128(4)
α (deg)	90	90	61.958(3)	90
β (deg)	96.893(2)	90	84.894(3)	93.04(3)
γ (deg)	90	90	85.547(3)	90
V (Å^3)	2495.1(3)	5381.9(2)	5890(3)	5726(2)
Z	4	4	1	4
μ(Mo Kα) (mm^{-1})	0.764	0.715	0.272	0.280
crystal size (mm)	0.15 × 0.12 × 0.08	0.26 × 0.19 × 0.12	0.20 × 0.25 × 0.30	0.20 × 0.10 × 0.08
F (000)	1188	2528	2228	2268
2θ range (deg)	1.60−28.87	1.63−36.17	1.005−24.376	2.54−24.92
T (K)	100(1)	100(1)	273(2)	123(2)
number of data collected	10559	109804	30649	15829
number of unique data	5267	23697	30649	8068
observed data [$I > 2\sigma(I)$] (N_o)	4220	20393	10632	2683
Rint (%)	1.82	2.89	0	12.7
number of parameters (N_p)	316	680	2809	809
R_1 (%)[a]	5.54	3.51	7.94	11.54
wR_2 (%)[b]	15.78	8.49	9.71	24.74
S[c]	1.027	1.018	1.0730	0.923
$\Delta\rho_{min}$ (e$^-$ Å^{-3})	−0.683	−0.437	−1.12	−0.522
$\Delta\rho_{max}$ (e$^-$ Å^{-3})	1.172	0.690	2.10	0.987

[a] $R_1 = \sum||F_o| - |F_c||/\sum|F_o|$. [b] $wR_2 = \{\sum[w(F_o^2 - F_c^2)^2]/\sum[w(F_o^2)^2]\}^{1/2}$ and $w = 1/[\sigma^2(F_o^2) + (aP)^2 + bP]$ with $P = [F_o^2 + 2F_c^2]/3$, $a = 0.1537$ (for **1**) and 0.0353 (for **2**), and $b = 0.8654$ (for **1**) and 3.6214 (for **2**). [c] Goodness of fit $= [\sum w(|F_o| - |F_c|)^2/(N_o - N_p)]^{1/2}$.

and $NaBPh_4$ as starting materials and led to 1.8 g (yield = 82%) of a white precipitate. Crystallization of complex **3** was performed by slow diffusion of ether in a methanol solution of **3**, and crystals of **3**(BPh_4)$_2$ suitable for X-ray crystallography study were obtained. Anal. Calcd for **3**(BPh_4)$_2$·2H_2O (powder) $C_{69}H_{71}MnN_5B_2O_3$: C, 75.7; H, 6.5; N, 6.4. Found: C, 75.6; H, 6.3; N, 6.7. IR: ν (cm^{-1}) = 3440 (S, strong); 3035 (S); 2962 (w, weak); 1948 (w); 1824 (w); 1604 (S); 1570 (m, medium); 1483 (S); 1464 (S); 1442 (m); 1368 (w); 1307 (m); 1262 (m); 1157 (m); 1131 (m); 1082 (m); 1017 (S); 842 (m); 734 (S); 705 (S); 611 (S); 469 (S); 411 (m). ESI-MS: A major peak was detected at m/z = 201 corresponding to [(L_5^2)Mn]$^{2+}$.

[(L_5^3)Mn(OH_2)](BPh_4)$_2$·H_2O (4(BPh_4)$_2$·H_2O). An identical synthesis was performed using the ligand L_5^3 as starting material leading to 1.7 g (yield = 78%) of a white precipitate. Crystallization of complex **4** was performed by slow diffusion of methanol in an acetonitrile solution of **4**, and crystals of **4**(BPh_4)$_2$ suitable for X-ray crystallography study were obtained. Anal. Calcd for **4**(BPh_4)$_2$·H_2O (powder) $C_{70}H_{71}MnN_5B_2O_2$: C, 77.1; H, 6.6; N, 6.4. Found: C, 77.3; H, 6.3; N, 6.5. IR: ν (cm^{-1}) = 3450 (S, strong); 3050 (m, medium); 1605 (S); 1573 (w, weak); 1483 (S); 1471 (S); 1434 (S); 1377 (w); 1298 (m); 1220 (w); 1197 (w); 1137 (w); 1102 (w); 1055 (m); 1017 (m); 949 (w); 837 (w); 773 (S); 642 (S); 557 (S). ESI-MS: A major peak was detected at m/z = 208 corresponding to [(L_5^3)Mn]$^{2+}$.

Infrared Spectroscopy. The spectrum was recorded on KBr pellets in the range from 4000 to 400 cm^{-1} with a Perkin-Elmer Spectrum 1000 spectrophotometer.

Electrospray Ionization Mass Spectrometry. The mass spectra were recorded with a Finnigan Mat95 in a BE configuration at low resolution on micromolar acetonitrile solution.

Elemental Analysis. The analysis was performed by the Service de Microanalyse of the CNRS (Gif-sur-Yvette, France) for carbon, nitrogen, and hydrogen.

X-ray Crystallography. Crystal data for complexes **1**(PF_6), **2**(PF_6)·0.5CH_3CN, **3**(BPh_4)$_2$, **4**(BPh_4)$_2$ and the parameters of data collection are summarized in Table 1. Crystal data for **3**(BPh_4)$_2$ and **4**(BPh_4)$_2$ were collected on a Nonius Kappa-CCD area detector diffractometer using graphite-monochromated Mo Kα radiation (at Institut de Chimie des Substances Naturelles, UPR 2301, CNRS, 91198 Gif-sur-Yvette Cedex, France for complex **3** and at SCM, CEA/Saclay, Bât. 125, 91191 Gif-sur-Yvette Cedex, France for complex **4**). Crystal data for **1**(PF_6) and **2**(PF_6)·0.5CH_3CN were collected on a Bruker Kappa-X8 APEXII area detector diffractometer using graphite-monochromated Mo Kα radiation at ICMMO, UMR 8182, Université Paris-Sud, 91405 Orsay Cedex, France. The temperature of the crystal for **1**(PF_6), **2**(PF_6)·0.5CH_3CN, and **4**(BPh_4)$_2$ was maintained at the selected value (100 K for **1** and **2** or 123 K for **4**) by means of a 700 series Cryostream cooling device to within an accuracy of ± 1 K.

Data were corrected for Lorentz-polarization. The structures were solved by the direct methods with SHELXS-97[30] and refined by full matrix least-squares on F^2 with anisotropic thermal parameters for all non-H atoms with SHELXL-97.[31] H atoms were found in a difference Fourier map and were introduced at calculated positions as riding atoms, with C−H bond lengths of 0.93 (aromatic CH), 0.98 (aliphatic CH), 0.97 (CH_2), and 0.96 Å (CH_3), and with U_{iso}(H) values of 1.2U_{eq}(C) for CH- and CH_2-H atoms, and 1.5U_{eq}(C) for CH_3-H atoms. The drawing of the molecule was realized with the help of the Oak Ridge Thermal Ellipsoid Plot (ORTEP) program ORTEP32 for PC.[32] Crystallographic data for the structure reported in this paper have been deposited with the Cambridge Crystallographic Data Center, CCDC nos. 633240, 633241, 633242, and

(30) Sheldrick, G. M. *SHELXS-97: Program for crystal structure solution*; University of Göttingen: Göttingen, Germany, 1997.
(31) Sheldrick, G. M. *SHELXL-97: Program for refinement of crystal structures from diffraction data*, University of Göttingen: Göttingen, Germany, 1997.
(32) Ferrugia, L. J. *J. Appl. Crystallogr.* **1997**, *30*, 565.

633243. Copies of this information may be obtained free of charge from The Director, CCDC, 12 Union Road, Cambridge, CB2 1EZ, U.K. (fax: +44−1223−336033; e-mail: deposit@ccdc.cam.ac.uk or http://www.ccdc.cam.ac.uk).

HF-EPR Spectroscopy. HF-EPR spectra were recorded on a laboratory made spectrometer[33,34] using powder samples pressed in pellets to avoid preferential orientation of the crystallites in the strong magnetic field. A Gunn diode operating at 95 GHz and equipped with a third-harmonic generator has been used as the radiation source. The magnetic field was produced by a superconducting magnet (0−12 T).

The simulation of the HF-EPR spectra was performed using the SIM program written by Weihe.[15] It proceeds by full-matrix diagonalization of the spin Hamiltonian and includes the Boltzmann population factor for the calculation of transition probabilities.

Theoretical Calculations. All calculations reported in this work were performed with the ORCA program package.[35] When specified, the structures of the complexes were fully optimized using the BP86 functional[36,37] and the TZVP basis set.[38] For molecules lacking in the X-ray files the hydrogen atoms of the coordinated water molecule, namely, for **3**$(BPh_4)_2$, **4**$(BPh_4)_2$, and $[(L_6^2)\text{-}Mn(OH_2)](ClO_4)_2$, three, four and three sets, respectively, of coordinates were calculated based on the same O−H bond length and Mn−O−H and H−O−H bond angles as those in $[(L_4^3)MnCl(OH_2)](ClO_4)$. With this simplified view of the crystallographic snapshot, different complexes were thus constructed where, for the same compound, the orientation of the water molecule differs relative to the unchanged $L_5^{2/3}$−Mn fragment. EPR properties were calculated using spin-unrestricted DFT together with the spin−orbit meanfield (SOMF)[39] representation of the spin−orbit coupling (SOC) operator in the implementation previously described in the literature.[40] For the calculation of the spin−spin contribution to the ZFS we refer to the work of Neese[41] while the SOC contribution was calculated with the method of Pederson and Khanna.[42]

Results and Discussion

We have prepared four mononuclear Mn^{II} complexes obtained with the pentadentate ligands L_5^2 and L_5^3 (see Chart 1).

With such pentadentate ligands built on 1,2-diaminoethane and 1,3-diamino-propane bridges, three different isomers are possibly accessible depending on the relative position of the pyridine rings as it is shown in Scheme 2. The isomer *fac* refers to a facial arrangement of the three pyridine functions, and the isomer *mer* to a meridional one. In the latter case, the relative position of the two pyridine functions anchored on the same amino nitrogen atom leads to two isomers. When the two pyridine functions anchored on the same amino nitrogen atom are in *cis* position then the isomer is named *mer-cis*, otherwise *mer-trans*.

Scheme 2. Different Configurations of the Pentadentate Ligands with the Nomenclature Used

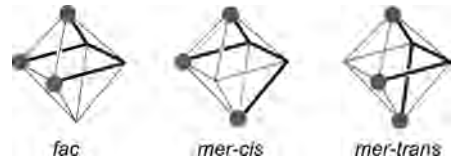

X-ray Crystal Structures of Mononuclear Complexes 1 to 4. ORTEP views of the four cations **1**−**4** are shown in Figure 1, and selected bond lengths and angles are given in Table 2. In all complexes, the Mn^{II} ion is wrapped by the pentadentate ligand and the coordination sphere is completed by an exogenous ligand, either a chloride ion (**1** and **2**) or a water molecule (**3** and **4**). Both the L_5^2 and L_5^3 ligands can adopt two configurations either *mer-cis* in **1** and **2** or *mer-trans* in **3** and **4.** Therefore, no direct relation between the lengths of the diamino bridge (2 or 3 carbon linker) and the configuration of the ligand can be drawn. It is observed that the configuration of the ligand depends on the exogenous ligand and/or the counterion. Angles reported in Table 2 show that the departure from the regular octahedron is enhanced in complexes **1** and **3** and has to be related to the constraint imposed by the five-membered diamino bridge metallacycle. Indeed, replacement of L_5^2 by L_5^3 allows the $N_{a1}-Mn-N_{a2}$ angle to increase from 77.49(10)° to 93(2)° in the case of the chloro complexes **1** and **2**. A similar increase has been previously observed for the analogous Fe^{II} cation, namely $[(L_5^2)FeCl]^{+}$[43] and $[(L_5^3)FeCl]^{+}$.[27] The variation of the $N_{a1}-Mn-N_{a2}$ angle is also present in the case of the aqua complexes **3** and **4** (from 80.46(30)° to 97.76(70)°).

The Mn−Cl bonds in **1** and **2** are longer than the corresponding $Mn-OH_2$ bonds in **3** and **4**. The lengthening is less pronounced between **2** and **4** than between **1** and **3**, for which a more adjustable coordination sphere has been anticipated. Bulkiness of the chloride ion compared to that of the aqua ligand is thus responsible for such a difference. For the two chloro complexes, the Mn−Cl bond length (2.3757(9) and 2.422(17) Å for **1** and **2**, respectively) is

(33) Barra, A.-L.; Brunel, L.-C.; Robert, J. B. *Chem. Phys. Lett.* **1990**, *165*, 107–109.
(34) Muller, F.; Hopkins, M. A.; Coron, N.; Grynberg, M.; Brunel, L.-C.; Martinez, G. *Rev. Sci. Instrum.* **1989**, *60*, 3681–3684.
(35) Neese, F. *ORCA - An ab Initio, Density Functional and Semiempirical Program Package*, version 2.4.55; Universität Bonn: Bonn, Germany.
(36) Becke, A. D. *Phys. Rev. A* **1988**, *38*, 3098–3100.
(37) Perdew, J. P. *Phys. Rev B.* **1986**, *33*, 8822–8824.
(38) Schäfer, A.; Huber, C.; Ahlrichs, R. *J. Chem. Phys.* **1994**, *100*, 5829–5835.
(39) Heβ, B. A.; Marian, C. M.; Wahlgren, U.; Gropen, O. *Chem. Phys. Lett.* **1996**, *251*, 365–371.
(40) Neese, F. *J. Chem. Phys.* **2005**, *122*, 034107.
(41) Neese, F. *J. Am. Chem. Soc.* **2006**, *128*, 10213–10222.
(42) Pederson, M. R.; Khanna, S. N. *Phys. Rev B.* **1999**, *60*, 9566–9572.
(43) Mialane, P.; Nivorojkine, A.; Pratviel, G.; Azéma, L.; Slany, M.; Godde, F.; Simaan, A.; Banse, F.; Kargar-Grisel, T.; Bouchoux, G.; Sainton, J.; Horner, O.; Guilhem, J.; Tchertanova, L.; Meunier, B.; Girerd, J.-J. *Inorg. Chem.* **1999**, *38*, 1085–1092.
(44) Brudenell, S. J.; Spiccia, L.; Bond, A. M.; Fallon, G. D.; Hockless, D. C. R.; Lazarev, G.; Mahon, P. J.; Tiekink, E. R. T. *Inorg. Chem.* **2000**, *39*, 881–892.
(45) Collinson, S.; Alcock, N. W.; Raghunathan, A.; Kahol, P. K.; Busch, D. H. *Inorg. Chem.* **2000**, *39*, 757–764.
(46) El Ghachtouli, S.; Mohamadou, A.; Barbier, J.-P. *Inorg. Chim. Acta* **2005**, *358*, 3873–3880.
(47) Ghosh, K.; Eroy-Reveles, A. A.; Avila, B.; Holman, T. R.; Olmstead, M. M.; Mascharak, P. K. *Inorg. Chem.* **2004**, *43*, 2988–2997.
(48) Klein Gebbink, R. J. M.; Jonas, R. T.; Goldsmith, C. R.; Stack, T. D. P. *Inorg. Chem.* **2002**, *41*, 4633–4641.
(49) Lah, M. S.; Chun, H. *Inorg. Chem.* **1997**, *36*, 1782–1785.
(50) Li, Q.-X.; Luo, Q.-H.; Li, Y.-Z.; Pan, Z.-Q.; Shen, M.-C. *Eur. J. Inorg. Chem.* **2004**, 4447–4456.
(51) Wittmann, H.; Raab, V.; Schorm, A.; Plackmeyer, J.; Sundermeyer, J. *Eur. J. Inorg. Chem.* **2001**, 1937–1948.

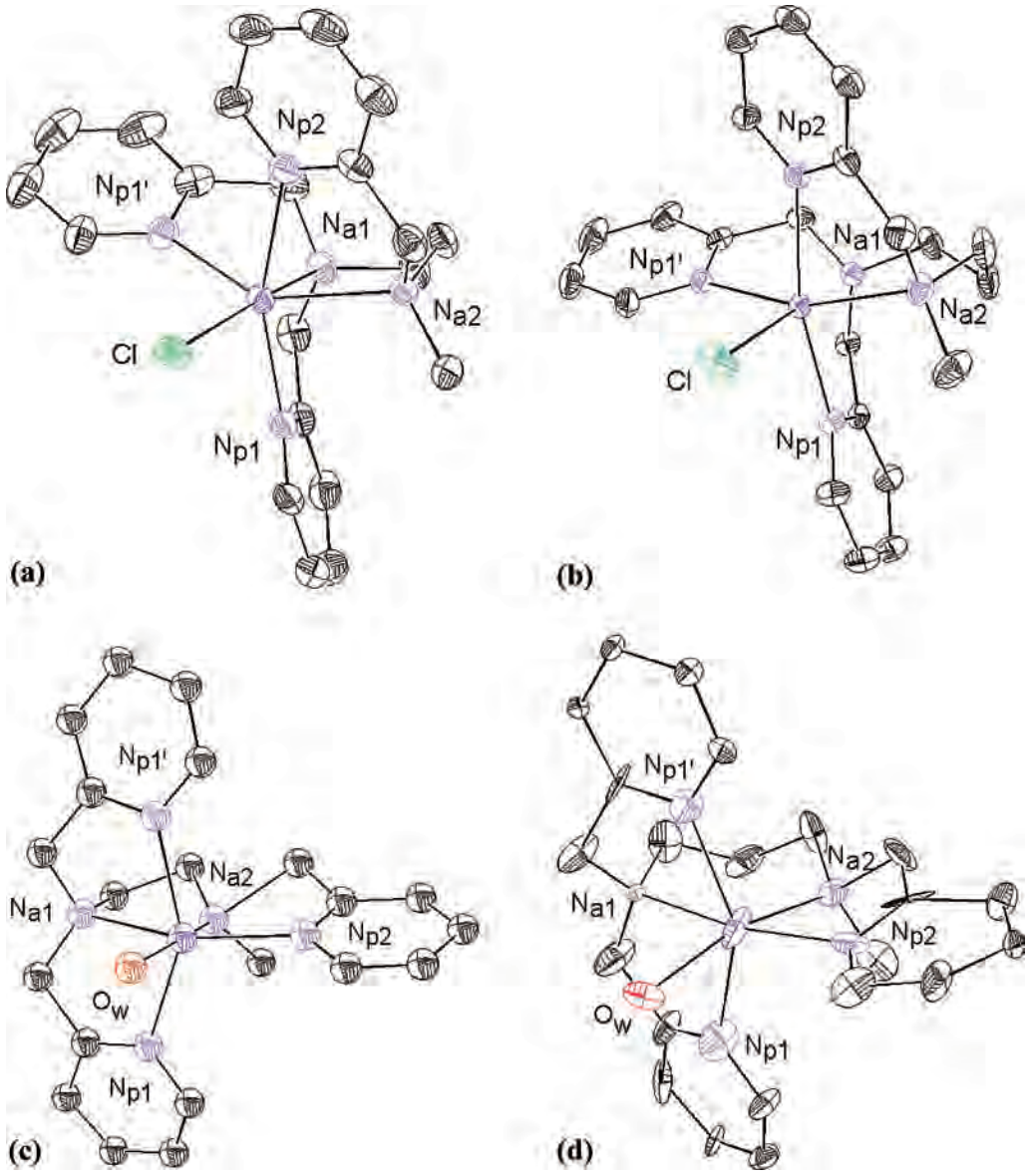

Figure 1. ORTEP drawings of the cations **1** (a), **2** (b), **3** (c), and **4** (d) with the ellipsoids drawn at the 50%, 50%, 30%, and 20% probability levels, respectively.

consistent with those of related complexes with [N_5Cl] donor set for which bond length values are reported between 2.35 and 2.53 Å.[44−51]

In the two aqua complexes **3** and **4**, Mn−OH_2 bond lengths (2.212(15) and 2.383(14) Å, respectively) are longer than those reported for other complexes with [N_5] donor sets and one coordinated water molecule (between 2.09 and 2.11 Å).[52−54] For all complexes the Mn−$N_{pyridine}$ bond lengths as well as the Mn−N_{amine} ones are within the range of literature data (2.1−2.4 Å).[18,25,44−48,50,52−55]

Solid State HF-EPR and DFT Investigations. A high spin Mn^{II} (d^5) ion is characterized by a fundamental electronic spin S of 5/2 and a nuclear spin I of 5/2. Its electronic properties can be described by the following Hamiltonian:

$$H = \mu_B \hat{B} \cdot \boldsymbol{g} \cdot \hat{S} + \hat{I} \cdot \mathbf{A} \cdot \hat{S} + D\left[\left(\hat{S}_z^2 - \frac{1}{3}S(S+1)\right) + \frac{E}{D}(\hat{S}_x^2 - \hat{S}_y^2)\right] \quad (1)$$

where the first term describes the electronic Zeeman effect and the second one the hyperfine interaction between the unpaired electrons and the Mn nucleus. The last term corresponds to the ZFS interaction and is described by the D and E parameters known as the axial and rhombic ZFS parameters, respectively (E/D defines the rhombicity). For high-spin Mn^{II} systems, the Zeeman effect is close to isotropy with the three principal values of the g-matrix close to 2. When the Zeeman effect largely dominates against the ZFS, the latter interaction can be treated by perturbation theory at first order. It is typically the case when the spectrum is

(52) de Vries, M. E.; La Crois, R. M.; Roelfes, G.; Kooijman, H.; Spek, A. L.; Hage, R.; Feringa, B. L. *Chem. Commun.* **1997**, 1549–1550.
(53) Goldsmith, C. R.; Cole, A. P.; Stack, T. D. P. *J. Am. Chem. Soc.* **2005**, *127*, 9904–9912.
(54) Sreerama, S. G.; Pal, S.; Pal, S. *Inorg. Chem. Commun.* **2001**, *4*, 656–660.
(55) Blanchard, S.; Blondin, G.; Rivière, E.; Nierlich, M.; Girerd, J.-J. *Inorg. Chem.* **2003**, *42*, 4568–4578.

Table 2. Selected Bond Lengths (Å) and Angles (deg) for the Cations **1**, **2**, **3**, and **4**

	1	**2**[a]		**3**[b]	**4**
$Mn-N_{a1}$	2.328(3)	2.348(18)	$Mn-N_{a2}$	2.223(17)	2.260(13)
$Mn-N_{a2}$	2.328(3)	2.316(19)	$Mn-N_{p2}$	2.226(15)	2.176(18)
$Mn-N_{p1}$	2.274(3)	2.235(6)	$Mn-N_{p1}$	2.264(14)	2.239(20)
$Mn-N_{p1'}$	2.246(3)	2.225(11)	$Mn-N_{a1}$	2.314(13)	2.246(18)
$Mn-N_{p2}$	2.340(3)	2.263(35)	$Mn-N_{p1'}$	2.265(16)	2.278(17)
Mn−Cl	2.3757(9)	2.422(17)	$Mn-OH_2$	2.212(15)	2.383(14)
$Cl-Mn-N_{a2}$	115.06(8)	96.36(4)	OH_2-Mn-N_{p2}	99.22(40)	91.13(60)
$N_{a2}-Mn-N_{a1}$	77.49(10)	93(2)	$N_{p2}-Mn-N_{a2}$	76.12(30)	79.18(60)
$N_{a1}-Mn-N_{p1'}$	72.21(10)	73.7(9)	$N_{a2}-Mn-N_{a1}$	80.46(30)	97.76(70)
$N_{p1'}-Mn-Cl$	99.72(8)	98(2)	$N_{a1}-Mn-OH_2$	103.93(40)	93.15(60)
$Cl-Mn-N_{p1}$	97.11(8)	95(2)	OH_2-Mn-N_{p1}	92.70(40)	86.13(60)
$N_{a2}-Mn-N_{p1}$	90.14(11)	96.1(7)	$N_{p2}-Mn-N_{p1}$	112.79(40)	98.80(60)
$N_{a1}-Mn-N_{p1}$	72.96(10)	76.00(8)	$N_{a2}-Mn-N_{p1}$	90.79(30)	104.19(70)
$N_{p1'}-Mn-N_{p1}$	104.45(11)	96(1)	$N_{a1}-Mn-N_{p1}$	74.38(30)	73.53(60)
$Cl-Mn-N_{p2}$	94.48(8)	93.6(3)	$OH_2-Mn-N_{p1'}$	87.54(30)	83.34(60)
$N_{a2}-Mn-N_{p2}$	71.95(10)	74.04(5)	$N_{p2}-Mn-N_{p1'}$	98.40(30)	109.41(70)
$N_{a1}-Mn-N_{p2}$	98.25(11)	96(1)	$N_{a2}-Mn-N_{p1'}$	91.37(30)	91.28(70)
$N_{p1'}-Mn-N_{p2}$	87.57(10)	91.6(7)	$N_{a1}-Mn-N_{p1'}$	74.82(30)	79.08(60)
$Cl-Mn-N_{a1}$	164.54(8)	167.42(4)	OH_2-Mn-N_{a2}	175.01(40)	166.72(70)
$N_{a2}-Mn-N_{p1'}$	140.34(11)	159.9(2)	$N_{p2}-Mn-N_{a1}$	155.47(40)	170.92(70)
$N_{p1}-Mn-N_{p2}$	161.58(10)	167(2)	$N_{p1}-Mn-N_{p1'}$	148.31(40)	149.99(70)

[a] Values averaged on the 2 molecules, angles values of the 2 molecules being significantly distinct. [b] Values averaged on the 4 molecules.

Table 3. ZFS Parameters Obtained from the 285 GHz HF-EPR Spectra and from DFT Calculations[a]

compound		experiment[b]			DFT calculations[b]			
formula	sphere	D_{exp}	E_{exp}	$(E/D)_{exp}$	D_{calc}	E_{calc}	$(E/D)_{calc}$	$\lvert D_{calc}/D_{exp}\rvert$
cis-[(L_4^2)$MnCl_2$]	N_4Cl_2	−0.147	−0.021	0.14	−0.120	−0.036	0.30	0.82
cis-[(tpa)$MnCl_2$][c] [18]	N_4Cl_2	+0.115	+0.023	0.20	+0.155	+0.026	0.17	1.35
cis-[(phen)$_2MnCl_2$][d] [16]	N_4Cl_2	0.124[e]	0.005	0.04				
1(PF_6)	N_5Cl	0.180[f]	+0.060	0.33	+0.254	+0.017	0.07	1.41
2(PF_6)[g]	N_5Cl	+0.157	0	0	+0.227	+0.007	0.03	1.45
					+0.219	+0.016	0.07	1.39
[(L_4^3)$MnCl(OH_2)$](ClO_4)	N_4ClO	+0.110	+0.016	0.14	+0.150	+0.036	0.24	1.36
3$(BPh_4)_2$[h,I]	N_5O	−0.137	0	0	−0.089	−0.010	0.11	0.65
4$(BPh_4)_2$[h]	N_5O	−0.090	0	0	−0.080	−0.015	0.19	0.89
[(L_6^2)$Mn(OH_2)$]$(ClO_4)_2$[h]	N_6O	−0.127	0	0	−0.030	−0.005	0.17	0.24

[a] For comparison, two extra complexes are included. [b] The D and E parameters are given in cm^{-1}. [c] tpa is the tris(2-pyridylmethyl)amine ligand. [d] phen is the 1,10-phenanthroline ligand. [e] Undetermined sign for D. [f] The sign of D is meaningless because of the maximum rhombicity. [g] Calculations were performed on the two independent complexes present in the unit cell. [h] The reported values correspond to the average calculated on all the reconstituted complexes (see Experimental Section). [I] Calculations were performed on the Mn_1-containing complex.

recorded at high frequency and for small ZFS values (i.e., in high field limit conditions). In the present study, these conditions are satisfied as the recording frequency is 285 GHz (9.5 cm^{-1}) and the ZFS values determined inferior to 0.2 cm^{-1} (see Table 3). In the powder sample, the hyperfine interaction is presumably unresolved because of the intermolecular dipole−dipole interaction and contributes to the line width.

From a theoretical point of view, a $S = 5/2$ HF-EPR spectrum is the superimposition of the five m_S to $m_S + 1$ transitions, weighted by the Boltzmann population of each m_S level. At 285 GHz, two successive m_S levels are separated by 13.7 K. The m_S to $m_S + 1$ transitions are made of three components corresponding to the orientation of the magnetic field along the x, y, or z principal directions of the D tensor. However, a more intricate situation occurs for the central $m_S = -1/2$ to $m_S = +1/2$ transition. Because of weak anisotropies both in the Zeeman and ZFS interactions, features of the $m_S = -1/2$ to $m_S = +1/2$ transition are usually not resolved, and only one broad line is observed at $g = 2$. With respect to the position of this central line that can arbitrarily be shifted to zero, positions of the x, y, and z components of the four other transitions can be calculated.[17] At first order, these separations depend linearly on the ZFS parameters allowing the evaluation of D and E, both in sign and magnitude. Two simple cases are when the system is axial ($E/D = 0$) or completely rhombic ($E/D = 1/3$). In the former case, seven transitions located at $\pm 4|D|/g\mu_B$, $\pm 2|D|/g\mu_B$, $\pm|D|/g\mu_B$, and 0 (in field units) with respect to the center of the spectrum are expected at high temperature, while in the latter, five transitions located at $\pm 4|D|/g\mu_B$, $\pm 2|D|/g\mu_B$, and 0 (in field units) are expected. The sign of D is related to the position of the most distant component of the $m_S = -5/2$ to $m_S = -3/2$ transition from the center of the spectrum that can be well observed at low temperature in high field limit conditions. When this transition is on the low (respectively high) field edge then D is negative (respectively positive). It has to be noted that the sign of D in meaningless for E/D close to 1/3. For Mn^{II} systems, the Mn-hyperfine interaction must be taken into account. Indeed, a more intricate spectrum can be obtained in diluted samples, either solution samples,[56] magnetically diluted Mn^{II} powders,[57,58] or proteins.[20]

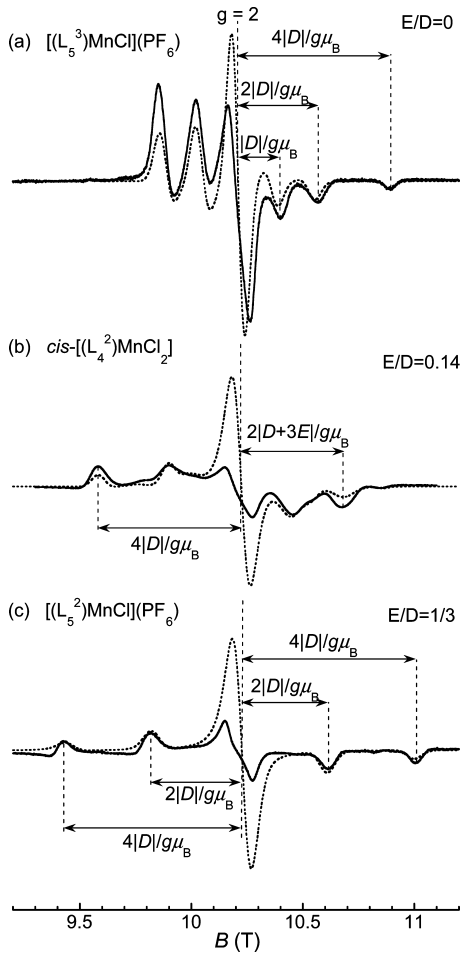

Figure 2. Experimental (solid line) and theoretical (dashed line) 285 GHz spectra of **2**$(PF_6)\cdot 0.5CH_3CN$, *cis*-$[(L_4^2)MnCl_2]$, and **1**(PF_6). $T = 30$ K. The spectra are classified with increasing rhombicity from the top to the bottom. The direct determination of the ZFS parameters (in field units) is indicated for each case.

Solid state HF-EPR spectra were recorded at 285 GHz for complexes **1**−**4** and for the three complexes *cis*-$[(L_4^2)MnCl_2]$, $[(L_4^3)MnCl(OH_2)]^+$, and $[(L_6^2)Mn(OH_2)]^{2+}$. The HF-EPR spectra of the three Mn^{II} compounds **1**(PF_6), **2**$(PF_6)\cdot 0.5CH_3CN$, and *cis*-$[(L_4^2)MnCl_2]$ are shown in Figure 2. These three spectra are representative of those obtained for the whole series. The spectrum widths are close whereas the patterns are clearly different, reflecting similar $|D|$ values and distinct E/D ratios for the three complexes. The two simplest spectra are characteristic of an axial (Figure 2a) and of a completely rhombic system (Figure 2c). Only six transitions out of the seven expected are observed for complex **2** because of unequal population of the five Zeeman levels at 30 K, while the spectrum of **1** displays the five expected transitions. The complex *cis*-$[(L_4^2)MnCl_2]$ corresponds to an intermediate case with a rhombicity of 0.14 in agreement with a more intricate spectrum (Figure 2b).

The experimental HF-EPR spectra were simulated (see Figure 2), and the parameters are listed in Table 3 for the whole series. The simulated HF-EPR spectra reproduced with a good agreement the field location as well as the shape of the experimental transitions, except for the central line certainly because of a saturation effect at low temperature. This problem is recurrent for mononuclear Mn^{II} complexes with slow electronic relaxation rates.[18,19,59] It may be noted that the E/D value for the chloro-complexes varies from 0 to 1/3 while all the N,O-coordinated complexes present an axial symmetry. The values obtained here for the heptacoordinated compound $[(L_6^2)Mn(OH_2)](ClO_4)_2$ are in agreement with those determined in our previous investigation at X-band ($|D| = 0.118$ cm^{-1} with $E/D = 0.03$ at 25 K).[25] To our knowledge, this is the only heptacoordinated mononuclear Mn^{II} complex investigated by EPR.

Table 3 gives the ZFS parameters issued from DFT calculations performed without structure optimization. Tables S2−S4 in the Supporting Information gather the results obtained on optimized structures. Both methods lead to similar values with the exception of *cis*-$[(L_4^2)MnCl_2]$. The structure optimization leads to a significant decrease in the Mn−Cl bond lengths (2.386 vs 2.451 Å) with a concomitant important increase in the Mn−N_{amine} bonds *trans* to the chloride ions (2.549 Å in average vs 2.366 Å). Similar variations in the metal−ligand distances were observed for the *cis*-$[(tpa)MnCl_2]$ complex.[60] Consequently, only the results of the calculations performed on complexes with the structures as determined from X-ray diffraction studies are presented here. The calculations performed on the two independent complexes present in the unit cell of compound **2**$(PF_6)\cdot 0.5CH_3CN$ give similar results. The same conclusion holds for compounds **3**$(BPh_4)_2$, **4**$(BPh_4)_2$, and $[(L_6^2)Mn(OH_2)](ClO_4)_2$, the tested orientations of the coordinated water molecule leading to identical ZFS parameters (see Experimental Section). Hence, only the average values are given.

Table 3 indicates that the D magnitudes for the monochloro complexes (0.110−0.180 cm^{-1}) stand in average in between that observed for *cis*-dichloro complexes (0.115−0.146 cm^{-1}) and that for *trans*-dichloro compounds (0.186−0.208 cm^{-1}).[14−16,18] To our knowledge, only one monochloro complex has been previously investigated by EPR, namely, the pentacoordinated compound $[(tmc)MnCl](BPh_4)\cdot CH_3CN$ (tmc = 1,4,8,11-tetramethyl-1,4,8,11-tetraazacyclotetradecane).[61] The D parameter was estimated between 0.2 and 0.4 cm^{-1} from its X-band EPR signature. The larger D value for $[(tmc)MnCl]^+$ compared to those of the monochloro complexes investigated here is imputable to the pentacoordination of the Mn^{II} ion.[19]

(56) Stich, T. A.; Lahiri, S.; Yeagle, G.; Dicus, M.; Brynda, M.; Gunn, A.; Aznar, C.; DeRose, V. J.; Britt, R. D. *Appl. Magn. Reson.* **2007**, *31*, 321–341.
(57) Mantel, C.; Philouze, C.; Collomb, M.-N.; Duboc, C. *Eur. J. Inorg. Chem.* **2004**, 3880–3886.
(58) Duboc, C.; Phoeung, T.; Jouvenot, D.; Blackman, A. G.; McClintock, L. F.; Pécaut, J.; Deronzier, A.; Collomb, M.-N. *Polyhedron* **2007**, *26*, 5243–5249.
(59) Duboc, C.; Astier-Perret, V.; Chen, H.; Pécaut, J.; Crabtree, R. H.; Brudvig, G. W.; Collomb, M.-N. *Inorg. Chim. Acta* **2006**, *359*, 1541–1548.
(60) Zein, S.; Duboc, C.; Lubitz, W.; Neese, F. *Inorg. Chem.* **2008**, *47*, 134–142.
(61) Bucher, C.; Duval, E.; Barbe, J.-M.; Verpeaux, J.-N.; Amatore, C.; Guilard, R.; Le Pape, L.; Latour, J.-M.; Dahaoui, S.; Lecomte, C. *Inorg. Chem.* **2001**, *40*, 5722–5726.

Table 4. Spin-Spin (D_{SS}) and Spin-Orbit Coupling (D_{SOC}) Contributions to the D Values (in cm^{-1}) Obtained from DFT Calculations (No Structural Optimization)

compound	D_{calc}	D_{SS}	D_{SOC}	D_{SOC} contributions	
cis-[$(L_4^2)MnCl_2$]	−0.120	−0.012	−0.108	αα	−0.018
				ββ	−0.063
				αβ	−0.053
				βα	+0.026
1(PF_6)	+0.254	+0.057	+0.196	αα	+0.048
				ββ	+0.092
				αβ	+0.090
				βα	−0.034
2$(PF_6)\cdot 0.5CH_3CN$[a]	+0.227	+0.026	+0.201	αα	+0.027
				ββ	+0.077
				αβ	+0.121
				βα	−0.024
	+0.219	+0.015	+0.204	αα	+0.024
				ββ	+0.076
				αβ	+0.128
				βα	−0.024
[$(L_4^3)MnCl(OH_2)$](ClO_4)	+0.150	+0.003	+0.147	αα	+0.037
				ββ	+0.062
				αβ	+0.065
				βα	−0.017
3$(BPh_4)_2$[b,c]	−0.089	−0.025	−0.064	αα	−0.016
				ββ	−0.002
				αβ	−0.037
				βα	−0.009
4$(BPh_4)_2$[b]	−0.080	−0.024	−0.056	αα	−0.015
				ββ	−0.003
				αβ	−0.029
				βα	−0.009
[$(L_6^2)Mn(OH_2)$]$(ClO_4)_2$[b]	−0.030	+0.018	−0.048	αα	+0.007
				ββ	0
				αβ	−0.053
				βα	−0.002

[a] Calculations were performed on the two independent complexes present in the unit cell. [b] The reported values correspond to the average determined on all the complexes in which the positions of the hydrogen atoms of the coordinated water molecule were calculated (see Experimental Section). [c] Calculations were performed on the Mn_1-containing complexes.

It has been proposed that the main contribution to the D value for *cis*- and *trans*-dihalide complexes is the spin−orbit coupling (SOC) part of the D tensor, the spin−spin (SS) contribution being non-negligible only for the chloro complexes. In addition the dominant contribution to the D_{SOC} part arises from a cross term between the Mn and halide SOC contributions.[18] Table 4 reports the SS and SOC contributions to the D tensor. It can be seen that D_{SS} may contribute up to 22% to the total D value for the chloro complexes. Four types of excitation have to be considered in the SOC part: the α→α and β→β transitions do not change the total electronic spin while the α→β and β→α lead to a decrease or increase of one unit, respectively. Only the α→β contribution is taken into account within a simple ligand field theory. Table 4 shows that the four classes of excitation present comparable magnitudes with partially canceling signs. A similar behavior was indeed obtained for the *cis*-[(tpa)$MnCl_2$] complex[60] and the *trans*-[$(NH_3)_4MnCl_2$] model system.[18] We thus may anticipate that the SOC of the chloride anion is mainly responsible for the D value in the monochloro complexes as well.

Table 3 also reports the ZFS parameters for complexes with mixed N,O-coordination sphere. As mentioned previously, only one series of this type[23] has been previously investigated where the Mn^{II} ion is surrounded by the three nitrogen atoms of a tridentate ligand on one hand and three oxygen atoms of monodentate ligands on the other, one being a water molecule. From the powder HF-EPR spectra, positive D values are expected. Unfortunately, only the quantity $(D^2+3E^2)^{1/2}$ is reported and the values vary between 0.09 and 0.11 cm^{-1}. The D values deduced here are negative and the magnitudes of the same order or even slightly larger (0.090 and 0.137 cm^{-1} for **3**$(BPh_4)_2$ and **4**$(BPh_4)_2$, respectively). These values exceed those encountered for biological hexacoordinated Mn^{II} systems such as concanavalin A (0.02−0.03 cm^{-1})[62] or azide bound SOD (0.05−0.07 cm^{-1}).[63] When no halides are linked to a synthetic hexacoordinated Mn^{II} ion and with the exception of the N_3O_3 systems mentioned above,[23] only O_6- or N_6-coordination spheres have been investigated.[15,22,23,64−70] The ligands used are either mono- or bidentate and the D magnitudes range from 0.004 to 0.085 cm^{-1}. However, larger D values, 0.175 and 0.219 cm^{-1}, are obtained with the Mn^{II} ion doped in [$Cd(bpa)_2$]$(ClO_4)_2$ and [$Zn(bpa)_2$]$(ClO_4)_2$ compounds, respectively, where bpa is the bis(2-pyridylmethyl)amine ligand.[71] It is worth noticing that the large D magnitudes are thus met when tri- or higher polydentate amino-pyridine ligands chelate the metal ion. Such a chelation leads to important geometric constraints around the Mn^{II} ions, especially in the ligand−metal−ligand angles, that can be at the origin of these important ZFS effects. This point is further supported by the comparison between L_5^2- and L_5^3-complexes since the smallest D values are observed for the L_5^3-based complexes that present the weaker distortions from regular octahedron. The influence of the ligand−metal−ligand bite angles is currently under investigation.

The investigated series allows to underpin the consequences of a single ligand substitution. As mentioned above, the substitution of the chloride anion by a water molecule goes with a change in the configuration of the pentadentate ligand $L_5^{2/3}$. The D magnitude as deduced from HF-EPR spectra for the monochloro complexes is undoubtedly larger than that of monoaqua complexes (see Table 3). This trend is reproduced by DFT calculation. A close inspection of Table 4 reveals a dramatic decrease in the SOC contribution, mainly in the β→β and α→β excitations. As a consequence, the SS part of the D tensor in the aqua-complexes is roughly a third of the total D value. This is a larger percentage than

(62) Carmieli, R.; Manikandan, P.; Epel, B.; Kalb (Gilboa) , A. J.; Schnegg, A.; Savitsky, A.; Möbius, K.; Goldfarb, D. *Biochemistry* **2003**, *42*, 7863–7870.
(63) Un, S.; Dorlet, P.; Voyard, G.; Tabares, L. C.; Cortez, N. *J. Am. Chem. Soc.* **2001**, *123*, 10123–10124.
(64) Woltermann, G. M.; Wasson, J. R. *Chem. Phys. Lett.* **1972**, *16*, 92–97.
(65) Woltermann, G. M.; Wasson, J. R. *Inorg. Chem.* **1973**, *12*, 2366–2370.
(66) Woltermann, G. M.; Wasson, J. R. *J. Phys. Chem.* **1973**, *77*, 945–949.
(67) Woltermann, G. M.; Wasson, J. R. *J. Magn. Reson.* **1973**, *9*, 486–494.
(68) Woltermann, G. M.; Wasson, J. R. *J. Phys. Chem.* **1974**, *78*, 45–49.
(69) Palmer, R. A.; Yang, M. C.-L.; Hempel, J. C. *Inorg. Chem.* **1978**, *17*, 1200–1203.
(70) Linga Raju, C.; Gopal, N. O.; Narasimhulu, K. V.; Lakshmana Rao, J.; Venkata Reddy, B. C. *Spectrochim. Acta, Part A* **2005**, *61*, 2181–2187.
(71) Glerup, J.; Goodson, P. A.; Hodgson, D. J.; Michelsen, K.; Nielsen, K. M.; Weihe, H. *Inorg. Chem.* **1992**, *31*, 4611–4616.

that observed in chloro systems. The important variation in the $\beta \rightarrow \beta$ SOC contribution originates in the modification of the occupation of the manganese 3d spin down orbitals. They present a higher occupation when the coordination sphere contains a chloride anion (38.1 ± 2 vs 34.7 ± 1%) because of the partial charge transfer between the negatively charged chloride ion and the positively charged metal center.

Substitution of one pyridine ligand in complexes **1** and **4** by a chloride anion leads to *cis*-$[(L_4^2)MnCl_2]$ and $[(L_4^3)MnCl(OH_2)]^+$, respectively. A decrease of the *D* magnitude is observed when going from **1** to *cis*-$[(L_4^2)MnCl_2]$ while this leads to an increase when starting from **4** to generate $[(L_4^3)MnCl(OH_2)]^+$, in both experimental and theoretical data. This difference originates from the addition of a second chloride anion in *cis* position in the first case while no chloride is present in complex **4**.

A previous DFT investigation on Mn^{II} complexes reveals that the *E*/*D* ratio can not be accurately reproduced.[60] This is partly due to the small values of both *E* and *D* magnitudes, a few hundredth and tenth of wavenumbers, respectively, that leads to an important uncertainty in the *E*/*D* ratios. However, the theoretical *E*/*D* value has to be considered when discussing the sign of the *D* parameter: it is meaningful only for *E*/*D* ratios weaker than 0.2.[60] From Table 3 it thus can be seen that the sign of *D* is correctly reproduced by DFT calculation within the series.

The magnitudes of the *D* parameters are satisfyingly reproduced for all complexes with the exception of the heptacoordinated complex $[(L_6^2)Mn(OH_2)]^{2+}$. The SS and SOC contributions are of opposite signs, contrarily to what is observed in the other complexes (Table 4). This is however not sufficient of explain the disagreement between experimental and theoretical *D* values. We are currently involved in the synthesis of heptacoordinated complexes, and we believe that their investigation by EPR spectroscopy would be an important point for implementing the ORCA program.

Concluding Remarks. EPR spectroscopy with recording frequencies ranging from 9 to 285 GHz was used to collect data on a series of mononuclear Mn^{II} complexes. Most of the ZFS parameters have been determined from solid state investigations. As we mentioned earlier, the target for the chemists is to use these values to infer the Mn^{II} coordination sphere. No systematic conclusion can be drawn yet. However, the collection of more data and their rationalization will probably help chemists to relate these electronic signatures to their chemical reactivity.

To date, no general correlation between the coordination sphere composition and the sign of *D* can be established: *cis*-dichloro N_4Cl_2 complexes present either positive or negative *D* values, as the hexacoordinated systems with mixed N,O coordination spheres. In this last series, this may be due to the difference in N/O ratio.

A tentative correlation between the coordination number and the magnitude of the *D* parameter can be undertaken. In the case of pentacoordinated systems, five compounds with chelation by N, O, or Cl ligands have been investigated: three synthetic complexes, namely $[(terpy)MnCl_2]$,[19] $[(terpy)Mn(NCS)_2]$,[19] $[(tBu_3\text{-}terpy)Mn(N_3)_2]$,[57] (terpy = 2,2′:6′,2″-terpyridine and tBu_3-terpy = 4,4′,4″-tri*tert*butyl-2,2′:6′,2″-terpyridine) and two metalloproteins, Mn-SOD[63] and manganese metalloglutathione transferase FosA with the fosfomycin substrate.[12] The *D* values are −0.26, −0.300, −0.250, 0.355, and 0.235 cm^{-1}, respectively. These values indicate that absolute *D* values are larger for penta- than for hexacoordined systems having mixed N,O-environment. They also suggest that pentacoordinated coordination spheres lead to larger *D* magnitudes than that of N_5Cl or N_4Cl_2 systems.

Although one can tentatively conclude that increasing the number of coordinated chloride anions in hexacoordinated systems leads to increasing absolute *D* values, this statement falls apart as demonstrated above if we consider in one the two N_6-complexes Mn^{II} doped in $[Cd(bpa)_2](ClO_4)_2$ and $[Zn(bpa)_2](ClO_4)_2$[71] that present *D* parameters similar to those of mono- or *trans*-dichloro systems and in two the *cis*-dichloro systems that exhibit absolute *D* values weaker than those of the monochloro complexes.[14−16,18]

These studies also evidenced that the ZFS spin quantities are sensitive to small variations in the environment of the metal ion, especially when the coordination sphere is only made of nitrogen and oxygen atoms. Progress along this line is required to correlate structure and reactivity for Mn^{II} active sites in proteins or in solutions.

Supporting Information Available: CIF files of the X-ray structures of complexes **1**−**4**, E_{SS}, E_{SOC}, E_{calc}, g_{iso}, and A_{iso} values obtained from DFT calculations performed on the seven complexes investigated here without structure optimization, DFT results starting from optimized structures, principal directions of the ZFS tensors obtained from DFT calculations. This material is available free of charge via the Internet at http://pubs.acs.org.

IC800551U